

PART 2.

Chemistry in High-Mass Star-Forming Regions

Chemistry in the Envelopes around Massive Young Stars

Ewine F. van Dishoeck and Floris F. S. van der Tak

Leiden Observatory, P.O. Box 9513, 2300 RA Leiden, The Netherlands

Abstract. Recent observational studies of intermediate- and high-mass star-forming regions at submillimeter and infrared wavelengths are reviewed, and chemical diagnostics of the different physical components associated with young stellar objects are summarized. Procedures for determining the temperature, density and abundance profiles in the envelopes are outlined. A detailed study of a set of infrared-bright massive young stars reveals systematic increases in the gas/solid ratios, the abundances of evaporated molecules, and the fraction of heated ices with increasing temperature. Since these diverse phenomena involve a range of temperatures from < 100 K to 1000 K, the enhanced temperatures must be communicated to both the inner and outer parts of the envelopes. This 'global heating' plausibly results from the gradual dispersion of the envelopes with time. Similarities and differences with low-mass YSOs are discussed. The availability of accurate physical models will allow chemical models of ice evaporation followed by 'hot core' chemistry to be tested in detail.

1. Introduction

Massive star-forming regions have traditionally been prime targets for astrochemistry owing to their bright molecular lines (e.g. Johansson et al. 1984; Cummins et al. 1986; Irvine et al. 1987; Ohishi 1997). Massive young stellar objects (YSOs) have luminosities of $\sim 10^4$ – $10^6 L_{\odot}$ and involve young O- and B-type stars. Because their formation proceeds more rapidly than that of low-mass stars and involves ionizing radiation, substantial chemical differences may be expected. The formation of high mass stars is much less well understood than that of low-mass stars. For example, observational phenomena such as ultracompact H II regions, hot cores, masers and outflows have not yet been linked into a single evolutionary picture. Chemistry may well be an important diagnostic tool in establishing such a sequence.

Most of the early work on massive star-forming regions has centered on two sources, Orion-KL and Sgr B2. Numerous line surveys at millimeter (e.g. Blake et al. 1987; Turner 1991) and submillimeter (Jewell et al. 1989; Sutton et al. 1991, 1995; Schilke et al. 1997) wavelengths have led to an extensive inventory of molecules through identification of thousands of lines. In addition, the surveys have shown strong chemical variations between different sources.

In recent years, new observational tools have allowed a more detailed and systematic study of the envelopes of massive YSOs. Submillimeter observations

routinely sample smaller beams (typically $15''$ vs. $30''$ – $1'$) and higher critical densities ($\geq 10^6$ vs. 10^4 cm^{-3}) than the earlier work. Moreover, interferometers at 3 and 1 millimeter provide maps with resolutions of $0.5''$ – $5''$. Finally, ground- and space-based infrared observations allow both the gas and the ices to be sampled (e.g. Evans et al. 1991; van Dishoeck et al. 1999). These observational developments have led to a revival of the study of massive star formation within the last few years. Recent overviews of the physical aspects of high-mass star formation are found in Churchwell (1999) and Garay & Lizano (1999).

In this brief review, we will first summarize available observational diagnostics to study the different phases and physical components associated with massive star formation. Subsequently, an overview of recent results on intermediate mass YSOs is given, which are often better characterized than their high-mass counterparts because of their closer distance. Subsequently, we will discuss a specific sample of embedded massive YSOs which have been studied through a combination of infrared and submillimeter data. After illustrating the modeling techniques, we address the question how the observed chemical variations are related to evolutionary effects, different conditions in the envelope (e.g. T , mass) or different luminosities of the YSOs. More extensive overviews of the chemical evolution of star-forming regions are given by van Dishoeck & Blake (1998), Hartquist et al. (1998), van Dishoeck & Hogerheijde (1999) and Langer et al. (2000). Schilke et al. (this volume) present high spatial resolution interferometer studies, whereas Macdonald & Thompson (this volume) focus on submillimeter data of hot core/ultracompact H II regions. Ices are discussed by Ehrenfreund & Schutte (this volume).

2. Submillimeter and Infrared Diagnostics

The majority of molecules are detected at (sub-)millimeter wavelengths, and line surveys highlight the large variations in chemical composition between different YSOs, both within the same parent molecular cloud and between different clouds. The recent 1–3 mm surveys of Sgr B2 (Nummelin et al. 1998; Ohishi & Kaifu 1999) dramatically illustrate the strong variations between various positions (see Figure 1). The North position is typical of ‘hot core’-type spectra, which are rich in lines of saturated organic molecules. This position has also been named the ‘large molecule heimat’ (e.g. Kuan & Snyder 1994; Liu & Snyder 1999). The Middle position has strong SO and SO₂ lines, whereas the Northwest position has a less-crowded spectrum with lines of ions and long carbon chains. A similar differentiation has been observed for three positions in the W 3 giant molecular cloud by Helmich & van Dishoeck (1997), who suggested an evolutionary sequence based on the chemistry.

The availability of complete infrared spectra from 2.4–200 μm with the *Infrared Space Observatory* (ISO) allows complementary variations in infrared features to be studied. Figure 2 shows an example of ISO–SWS and LWS spectra of two objects: Cep A ($L \approx 2.4 \times 10^4 L_{\odot}$) and S 106 ($L \approx 4.2 \times 10^4 L_{\odot}$). The Cep A spectrum is characteristic of the deeply embedded phase, in which the silicates and ices in the cold envelope are seen in absorption. The S 106 spectrum is typical of a more evolved massive YSO, with strong atomic and ionic lines in emission and prominent PAH features. A similar sequence has been shown

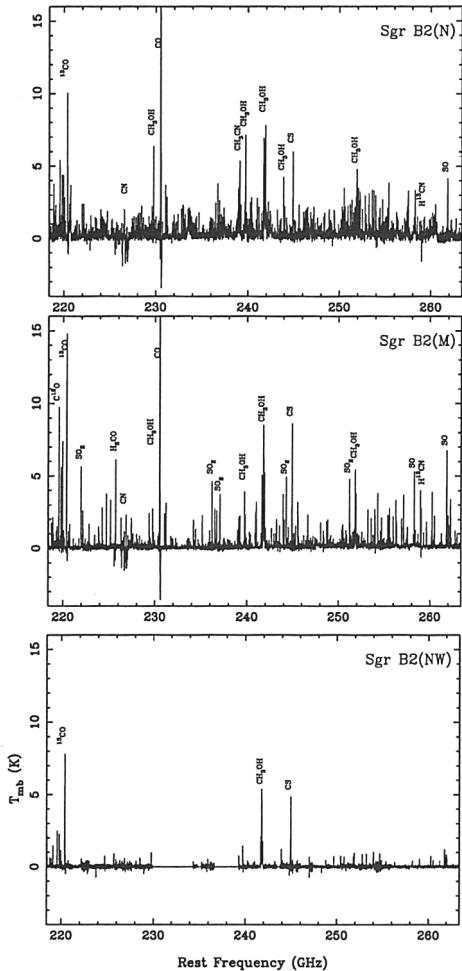


Figure 1. Overview of the SEST 230 GHz line survey of Sgr B2 at the N, M and NW positions, illustrating the chemical differentiation in high-mass star-forming regions (from: Nummelin et al. 1998).

by Ehrenfreund et al. (1998) for a set of southern massive young stars with luminosities up to $4 \times 10^5 L_{\odot}$.

The most successful models for explaining these different chemical characteristics involve accretion of species in an icy mantle during the (pre-)collapse phase, followed by grain-surface chemistry and evaporation of ices once the YSO has started to heat its surroundings (e.g. Millar 1997). The evaporated molecules subsequently drive a rapid high-temperature gas-phase chemistry for a period of $\sim 10^4$ – 10^5 yr, resulting in complex, saturated organic molecules (e.g. Charnley et al. 1992, 1995; Charnley 1997; Caselli et al. 1993; Viti & Williams 1999). The abundance ratios of species such as $\text{CH}_3\text{OCH}_3/\text{CH}_3\text{OH}$ and $\text{SO}_2/\text{H}_2\text{S}$ show strong variations with time, and may be used as ‘chemical clocks’ for a period of 5000–30,000 yr since evaporation. Once most of the envelope has cleared, the ultraviolet radiation can escape and forms a photon-dominated region (PDR) at the surrounding cloud material, in which molecules are dissociated into radicals

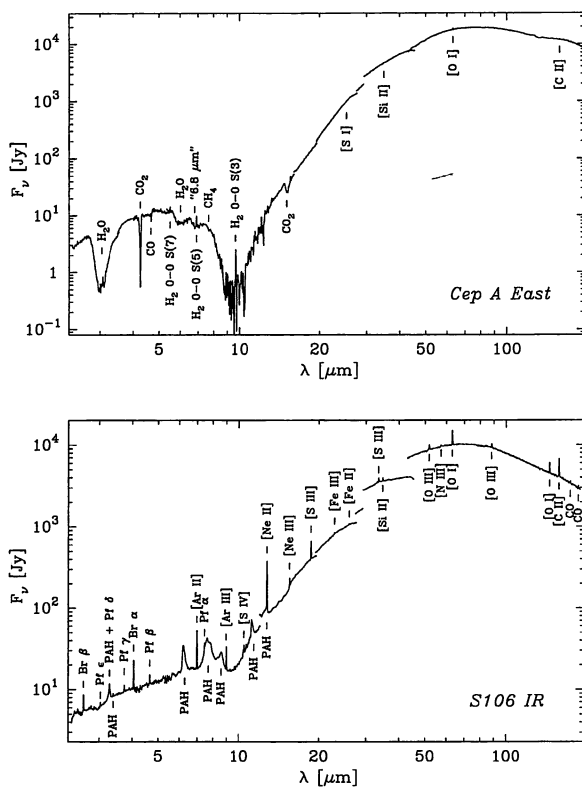


Figure 2. ISO-SWS spectra of two massive YSOs at different evolutionary stages. Cep A ($L \approx 2.4 \times 10^4 L_{\odot}$) is in the embedded stage, whereas S106 ($L \approx 4.2 \times 10^4 L_{\odot}$) is in a more evolved stage (from: van den Ancker et al. 2000a).

(e.g. $\text{HCN} \rightarrow \text{CN}$) and PAH molecules excited to produce infrared emission. The (ultra-)compact HII region gives rise to strong ionic lines due to photoionization.

Table 1 summarizes the chemical characteristics of the various physical components, together with the observational characteristics at submillimeter and infrared wavelengths. Within the single-dish submillimeter and ISO beams, many of these components are blended together and interferometer observations will be essential to disentangle them. Nevertheless, the single-dish data are useful because they encompass the entire envelope and highlight the dominant component in the beam. Combined with the above chemical scenario, one may then attempt to establish an evolutionary sequence of the sources.

The physical distinction between the ‘hot core’ and the warm inner envelope listed in Table 1 is currently not clear: does the ‘hot core’ represent a separate physical component or is it simply the inner warm envelope at a different stage of chemical evolution? Even from an observational point of view, there appear to be different types of ‘hot cores’: some of them are internally heated by the young star (e.g. $\text{W3}(\text{H}_2\text{O})$), whereas others may just be dense clumps of gas heated externally (e.g. the Orion compact ridge). This point will be further discussed

Table 1. Chemical characteristics of massive star-forming regions.

Component	Chemical characteristics	Submillimeter diagnostics	Infrared diagnostics	Examples
Dense cloud	Low-T chemistry	Ions, long-chains (HC ₅ N, ...)	Simple ices (H ₂ O, CO ₂)	Sgr B2 (NW)
Cold envelope	Low-T chemistry, Heavy depletions	Simple species (CS, H ₂ CO)	Ices (H ₂ O, CO ₂ , CH ₃ OH)	N7538 IRS9, W 33A
Inner warm envelope	Evaporation	High T _{ex} (CH ₃ OH)	High gas/solid, High T _{ex} , Heated ices (C ₂ H ₂ , H ₂ O, CO ₂)	GL 2591, GL 2136
Hot core	High-T chemistry	Complex organics (CH ₃ OCH ₃ , CH ₃ CN, vib. excited mol.)	Hydrides (OH, H ₂ O)	Orion hot core SgrB2(N), G34.3, W 3(H ₂ O)
Outflow: Direct impact	Shock chemistry, Sputtering	Si- and S-species (SiO, SO ₂)	Atomic lines, Hydrides ([S I], H ₂ O)	W 3 IRS5, SgrB2(M)
PDR, Compact H II regions	Photodissociation, Photoionization	Ions, radicals (CN/HCN, CO ⁺)	Ionic lines, PAHs ([NeII], [CII])	S 140, W 3 IRS4

in §§4 and 5. Disks are not included in Table 1, because little is known about their chemical characteristics, or even their existence, around high-mass YSOs (see Norris, this volume).

3. Intermediate-Mass YSOs

Intermediate-mass pre-main sequence stars, in particular the so-called Herbig Ae/Be stars, have received increased observational attention in recent years (see Waters & Waelkens 1998 for a review). These stars have spectral type A or B and show infrared excesses due to circumstellar dust. Typical luminosities are in the range 10^2 – 10^4 L_⊙, and several objects have been located within 1 kpc distance. Systematic mapping of CO and the submillimeter continuum of a sample of objects has been performed by Fuente et al. (1998) and Henning et al. (1998). The data show the dispersion of the envelope with time starting from the deeply embedded phase (e.g. LkHα234) to the intermediate stage of a PDR (e.g. HD 200775 illuminating the reflection nebula NGC 7023) to the more evolved stage where the molecular gas has disappeared completely (e.g. HD 52721). The increasing importance of photodissociation in the chemistry is probed by the increase in the CN/HCN abundance ratio. This ratio has been shown in other high-mass sources to be an excellent tracer of PDRs (e.g. Simon et al. 1997; Jansen et al. 1995). Line surveys of these objects in selected frequency ranges would be useful to investigate their chemical complexity, especially in the embedded phase.

ISO-SWS observations of a large sample of Herbig Ae/Be stars have been performed by van den Ancker et al. (2000b,c). In the embedded phase, shock indicators such as [S I] 25.2 μm are strong, whereas in the later phases PDR indicators such as PAHs are prominent. An excellent example of this evolutionary sequence is provided by three Herbig Ae stars in the BD+40°4124 region ($d \approx 1$ kpc). The data suggest that in the early phases, the heating of the envelope

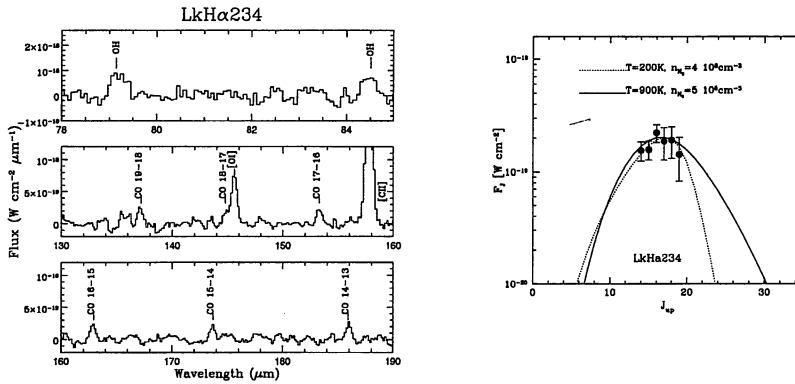


Figure 3. Left: ISO-LWS spectra of the intermediate mass YSO LkH α 234, showing strong atomic fine-structure lines of [C II] 158 μ m and [O I] 63 μ m, but weak molecular CO and OH lines. Right: CO excitation diagram, indicating the presence of a warm ($T \approx 200$ –900 K), dense ($n > 10^5 \text{ cm}^{-3}$) region (from: Giannini et al. 2000).

is dominated by shocks, whereas in later phases it is controlled by ultraviolet photons.

ISO-LWS data have been obtained for a similar sample of Herbig Ae/Be stars by Lorenzetti et al. (1999) and Giannini et al. (2000), and are summarized by Saraceno et al. (1999). The [C II] 158 μ m and [O I] 63 and 145 μ m lines are prominent in many objects and are due primarily to the PDR component in the large LWS beam ($\sim 80''$). High- J CO and OH far-infrared lines have been detected in some objects and indicate the presence of a compact, high temperature and density region of ~ 1000 AU in size, presumably tracing the inner warm envelope (see Figure 3). Far-infrared lines of H₂O are seen in low-mass YSO spectra, but are weak or absent in those of intermediate- and high-mass YSOs, with the exception of Orion-KL and Sgr B2 (e.g. Harwit et al. 1998; Cernicharo et al. 1997; Wright et al. 2000). The absence of H₂O lines in higher-mass objects may be partly due to the larger distance of these objects, resulting in substantial dilution in the LWS beam. However, photodissociation of H₂O to OH and O by the enhanced ultraviolet radiation may also play a role.

In summary, both the submillimeter and infrared diagnostics reveal an evolutionary sequence from the youngest ‘Group I’ objects to ‘Group III’ objects (cf. classification by Fuente et al. 1998), in which the envelope is gradually dispersed. Such a sequence is analogous to the transition from embedded Class 0/I objects to more evolved Class II/III objects in the case of low-mass stars (Adams et al. 1987). The ISO data provide insight into the relative importance of the heating and removal mechanisms of the envelope. At the early stages of intermediate-mass star formation, shocks due to outflows appear to dominate whereas at later stages radiation is more important.

4. Embedded, Infrared-Bright Massive YSOs

4.1. Sample

The availability of complete, high quality ISO spectra for a significant sample of massive young stars provides a unique opportunity to study these sources through a combination of infrared and submillimeter spectroscopy, and further develop these diagnostics. Van der Tak et al. (2000a) have selected a set of ~ 10 deeply embedded massive YSOs which are bright at mid-infrared wavelengths ($12\ \mu\text{m}$ flux > 100 Jy), have luminosities of $10^3 - 2 \times 10^5 L_{\odot}$ and distances $d \leq 4$ kpc. The sources are all in an early evolutionary state (comparable to the 'Class 0/I' or 'Group I' stages of low- and intermediate-mass stars), as indicated by their weak radio continuum emission and absence of ionic lines and PAH features. In addition to ISO spectra, JCMT submillimeter data and OVRO interferometer observations have been obtained. For most of the objects high spectral resolution ground-based infrared data of CO, ^{13}CO and H_3^+ are available (Mitchell et al. 1990; Geballe & Oka 1996; McCall et al. 1999), and occasionally H_2 (Lacy et al. 1994; Kulesa et al. 1999). For comparison, 5 infrared-weak sources with similar luminosities are studied at submillimeter wavelengths only. This latter set includes hot cores and ultracompact H II regions such as W 3(H_2O), IRAS 20126+4104 (Cesaroni et al. 1997, 1999), and NGC 6334 IRS1.

4.2. Physical structure of the envelope

In order to derive molecular abundances from the observations, a good physical model of the envelope is a prerequisite. Van der Tak et al. (1999, 2000a) outline the techniques used to constrain the temperature and density structure (Figure 4). The total mass within the beam is derived from submillimeter photometry, whereas the size scale of the envelope is constrained from line and continuum maps. The dust opacity has been taken from Ossenkopf & Henning (1994) and yields values for the mass which are consistent with those derived from C^{17}O for warm sources where CO is not depleted onto grains.

The temperature structure of the dust is calculated taking the observed luminosity of the source, given a power-law density structure (see below). At large distances from the star, the temperature follows the optically thin relation $\propto r^{-0.4}$, whereas at smaller distances the dust becomes optically thick at infrared wavelengths and the temperature increases more steeply (see Figure 5). It is assumed that $T_{\text{gas}} = T_{\text{dust}}$, consistent with explicit calculations of the gas and dust temperatures by, e.g., Doty & Neufeld (1997) for these high densities.

The continuum data are sensitive to temperature and column density, but not to density. Observations of a molecule with a large dipole moment are needed to subsequently constrain the density structure. One of the best choices is CS and its isotope C^{34}S , for which lines ranging from $J=2-1$ to $10-9$ have been observed. Assuming a power-law density profile $n(r) = n_o (r/r_o)^{-\alpha}$, values of α can be determined from minimizing χ^2 between the CS line data and excitation models. The radiative transfer in the lines is treated through a Monte-Carlo method. The best fit to the data on the infrared-bright sources is obtained for $\alpha = 1.0-1.5$, whereas the hot core/compact H II region sample requires higher values, $\alpha \approx 2$. This derivation assumes that the CS abundance is constant through the envelope; if it increases with higher temperatures, such as may be the case for hot

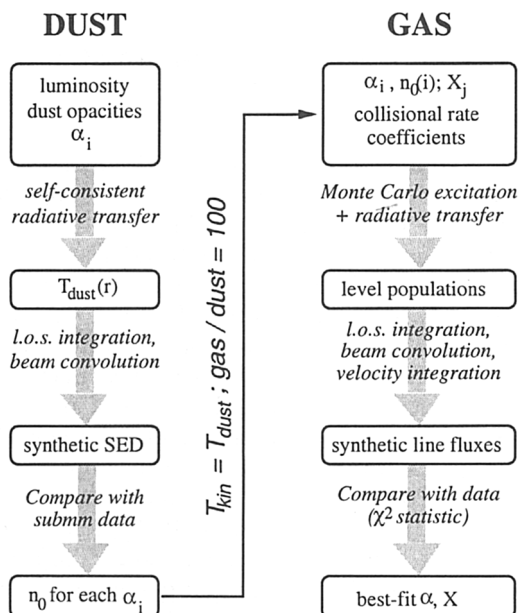


Figure 4. Overview of method used for constraining the temperature and density structure of envelopes. A power-law density structure with trial values for the exponent α_i and molecular abundances X_j is adopted (based on: van der Tak et al. 2000a).

cores, the values of α are lowered. Note that the derived values of $\alpha = 1.0$ – 1.5 are lower than those found for deeply embedded low-mass objects, where $\alpha \approx 2$ (e.g. Motte et al. 1998; Hogerheijde et al. 1999).

Figure 5 displays the derived temperature and density structure for the source GL 2591, together with the sizes of the JCMT and OVRO beams. While the submillimeter data are weighted toward the colder, outer envelope, the infrared absorption line observations sample a pencil-beam line of sight toward the YSO and are more sensitive to the inner warm (~ 1000 K) region. On these small scales, the envelope structure deviates from a radial power law, which decreases the optical depth at near-infrared wavelengths by a factor of ~ 3 (van der Tak et al. 1999).

For sources for which interferometer data are available, unresolved compact continuum emission is detected on scales of a few thousand AU or less. This emission is clearly enhanced compared with that expected from the inner “tip” of the power-law envelope, and its spectral index indicates optically thick warm dust, most likely in a dense circumstellar shell or disk. The presence of this shell or disk is also indicated by the prevalence of blue-shifted outflowing dense gas without a red-shifted counterpart on $< 10''$ scales.

4.3. Chemical structure: infrared absorption lines

The ISO-SWS spectra of the infrared-bright sources show absorption by various gas-phase molecules, in addition to strong features by ices. Molecules such as CO_2 (van Dishoeck et al. 1996, Boonman et al. 1999, 2000a), H_2O (van Dishoeck

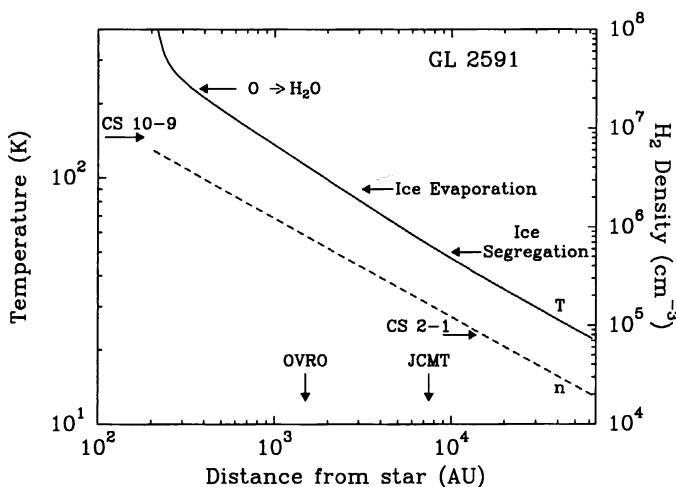


Figure 5. Derived temperature and density structure for the envelope around the massive YSO GL 2591 ($L = 2 \times 10^4 L_{\odot}$, $d = 1$ kpc). The critical densities of the CS 2-1 and 10-9 lines are indicated, as are the typical beam sizes of the JCMT at 345 GHz and OVRO at 100 GHz (based on: van der Tak et al. 1999).

& Helmich 1996; Boonman et al. 2000b), CH_4 (Boogert et al. 1998), HCN and C_2H_2 (Lahuis & van Dishoeck 2000) have been detected (see also van Dishoeck 1998; Dartois et al. 1998).

In the infrared, absorption out of all J -levels is observed in a single spectrum. The excitation temperatures T_{ex} of the various molecules, calculated assuming LTE, range from $\lesssim 100$ to ~ 1000 K between sources, giving direct information on the physical component in which the molecules reside. While CO is well-mixed throughout the envelopes, H_2O , HCN and C_2H_2 are enhanced at high temperatures. In contrast, CO_2 seems to avoid the hottest gas. High spectral resolution ground-based data of HCN and C_2H_2 by Carr et al. (1995) and Lacy et al. (1989) for a few objects suggest line widths of at most a few km s^{-1} , excluding an origin in outflowing gas.

The abundances of H_2O , HCN and C_2H_2 increase by factors of $\gtrsim 10$ with increasing T_{ex} (see Figure 7). The warm H_2O must be limited to a $\lesssim 1000$ AU region, since the pure rotational lines are generally not detected in the $80''$ ISO-LWS beam (Wright et al. 1997). For CO_2 , the abundance variation between sources is less than a factor of 10, and no clear trend with T_{ex} is found. For the same sources, the H_2O and CO_2 ice abundances show a decrease by an order of magnitude, consistent with evaporation of the ices. However, the gas-phase H_2O and CO_2 abundances are factors of ~ 10 lower than expected if all evaporated molecules stayed in the gas phase, indicating that significant chemical processing occurs after evaporation. More detailed modeling using the source structures derived from submillimeter data is in progress.

4.4. Chemical structure: submillimeter emission

The JCMT data of the infrared-bright objects show strong lines, but lack the typical crowded ‘hot core’ spectra observed for objects such as W 3(H_2O) and

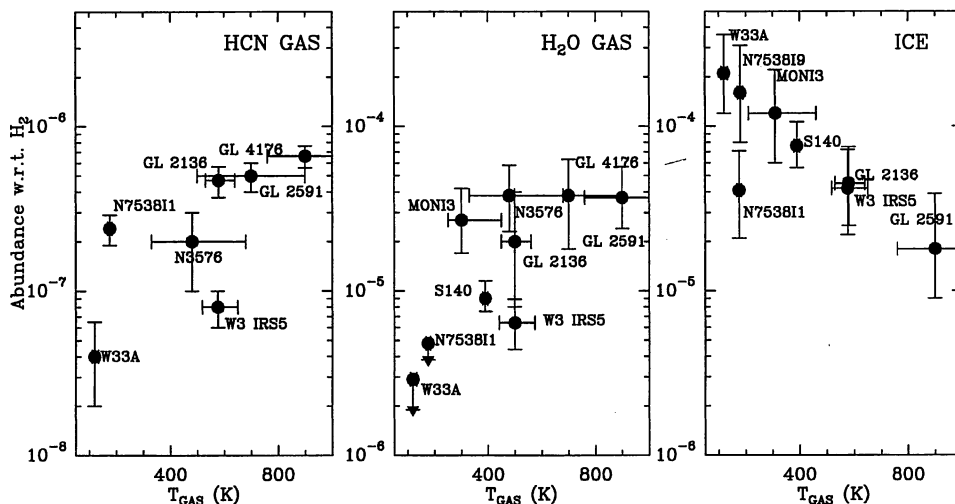


Figure 6. *Left:* Abundance of HCN, $N(\text{HCN})/N_{\text{tot}}(\text{H}_2)$, as a function of the ^{13}CO excitation temperature measured by Mitchell et al. (1990). *Middle:* Abundance of H_2O in the warm gas $N(\text{H}_2\text{O})/N_{\text{warm}}(\text{H}_2)$ as a function of ^{13}CO excitation temperature; *Right:* Abundance of H_2O ice as a function of ^{13}CO excitation temperature. The same trend is found if the dust temperature, as derived from the 45/100 μm flux, is used (based on: Lahuis & van Dishoeck 2000; van Dishoeck 1998).

NGC 6334 IRS1. Complex organics such as CH_3OCH_3 and CH_3OCHO are detected in some sources (e.g. GL 2591, NGC 7538 IRS1), but are not as prominent as in the comparison sources. Yet warm gas is clearly present in these objects. Is the ‘hot core’ still too small to be picked up by the single dish beams, or are the abundances of these molecules not (yet) enhanced?

To investigate this question, van der Tak et al. (2000b) consider the analysis of two species, H_2CO and CH_3OH . Both species have many lines throughout the submillimeter originating from low- and high-lying energy levels. Given the physical structure determined in §4.2, abundance profiles can be constrained. Two extreme, but chemically plausible models are considered: (i) a model with a constant abundance throughout the envelope. This model is motivated by the fact that pure gas-phase reaction schemes do not show large variations in calculated abundances between 20 and 100 K; (ii) a model in which the abundance ‘jumps’ to a higher value at the ice evaporation temperature, $T_d \approx 90$ K. In this model, the abundances in the outer envelope are set at those observed in cold clouds, so that the only free parameter is the amount of abundance increase.

It is found that the H_2CO data can be well fit with a constant abundance of a few $\times 10^{-9}$ throughout the envelope. However, the high J, K data for CH_3OH require a jump in its abundance from $\sim 10^{-9}$ to $\sim 10^{-7}$ for the warmer sources. This is consistent with the derived excitation temperatures: H_2CO has a rather narrow range of $T_{\text{ex}}=50\text{--}90$ K, whereas CH_3OH shows $T_{\text{ex}}=30\text{--}200$ K. Moreover, the interferometer maps of CH_3OH rule out constant abundance models. The

jump observed for CH₃OH is chemically plausible since this molecule is known to be present in icy grain mantles with abundances of 5–40% with respect to H₂O ice, i.e., $\sim 10^{-7}$ – 10^{-6} w.r.t. H₂. Similar increases in the abundances of organic molecules (e.g. CH₃OH, C₂H₃CN, ...) are found with increasing T_{dust} for a set of ‘hot-core’ objects by Ikeda & Ohishi (1999).

4.5. Comparison with chemical models

Both the infrared and submillimeter data show increases in the abundances of various molecules with increasing temperature. Four types of species can be distinguished: (i) ‘passive’ molecules which are formed in the gas phase, freeze out onto grains during the cold (pre-)collapse phase and are released during warm-up without chemical modification (e.g. CO, C₂H₂); (ii) molecules which are formed on the grains during the cold phase by surface reactions and are subsequently released into the warm gas (e.g. CH₃OH); (iii) molecules which are formed in the warm gas by gas-phase reactions with evaporated molecules (e.g. CH₃OCH₃); (iv) molecules which are formed in the hot gas by high temperature reactions (e.g. HCN). These types of molecules are associated with characteristic temperatures of (a) $T_{\text{dust}} < 20$ K, where CO is frozen out; the presence of CO ice is thought to be essential for the formation of CH₃OH; (b) $T_{\text{dust}} \approx 90$ K, where all ices evaporate on a time scale of $< 10^5$ yr; and (c) $T_{\text{gas}} > 230$ K, where gas-phase reactions drive the available atomic oxygen into water through the reactions $\text{O} + \text{H}_2 \rightarrow \text{OH} \rightarrow \text{H}_2\text{O}$ (Ceccarelli et al. 1996; Charnley 1997). Atomic oxygen is one of the main destroyers of radicals and carbon chains, so that its absence leads to enhanced abundances of species like HCN and HC₃N in hot gas.

Water is abundantly formed on the grains, but the fact that the H₂O abundance in the hot gas is not as large as that of the ices suggests that H₂O is broken down to O and OH after evaporation by reactions with H₃⁺. H₂O can subsequently be reformed in warm gas at temperatures above ~ 230 K, but Figure 7 indicates that not all available gas-phase oxygen is driven into H₂O, as the models suggest. The low abundance of CO₂ in the warm gas is still a puzzle, since evaporation of abundant CO₂ ice is observed. The molecule must be broken down rapidly in the warm gas, with no reformation through the CO + OH \rightarrow CO₂ reaction (see question by Minh).

4.6. Evolution ?

The objects studied by van der Tak et al. (2000a) are all in an early stage of evolution, when the young stars are still deeply embedded in their collapsing envelope. Nevertheless, even within this narrow evolutionary range, there is ample evidence for physical and chemical differentiation of the sources. This is clearly traced by the increase in the gas/solid ratios, the increase in abundances of several molecules, the decrease in the ice abundances, and the increase of the amount of crystalline ice with increasing temperature (Boogert et al. 2000a).

The fact that the various indicators involve different characteristic temperatures ranging from < 50 K (evaporation of apolar ices) to 1000 K (T_{ex} of gas-phase molecules) indicates that the heating is not a local effect, but that ‘global warming’ occurs throughout the envelope. Moreover, it cannot be a geometrical line-of-sight effect in the mid-infrared data, since the far-infrared

continuum (45/100 μm) and submillimeter line data (CH_3OH) show the same trend. Shocks with different filling factors are excluded for the same reason.

Can we relate this ‘global warming’ of the envelope to an evolutionary effect, or is it determined by other factors? The absence of a correlation of the above indicators with luminosity or mass of the source argues against them being the sole controlling factor. The only significant trend is found with the ratio of envelope mass over stellar mass. The physical interpretation of such a relation would be that with time, the envelope is dispersed by the star, resulting in a higher temperature throughout the envelope.

5. Outstanding Questions and Future Directions

The results discussed here suggest that the observed chemical abundance and temperature variations can indeed be used to trace the evolution of the sources, and that, as in the case of low- and intermediate-mass stars, the dispersion of the envelope plays a crucial role. The combination of infrared and submillimeter diagnostics is very important in the analysis. An important next step would be to use these diagnostics to probe a much wider range of evolutionary stages for high-mass stars, especially in the hot core and (ultra-)compact H II region stages, to develop a more complete scenario of high-mass star formation. The relation between the inner warm envelope and the ‘hot core’ is still uncertain: several objects have been observed which clearly have hot gas and evaporated ices (including CH_3OH) in their inner regions, but which do not show the typical crowded ‘hot core’ submillimeter spectra. Are these objects just on their way to the ‘hot core’ chemical phase? Or is the ‘hot core’ a separate physical component, e.g., a dense shell at the edge of the expanding hyper-compact H II region due to the pressure from the ionized gas, which is still too small to be picked up by the single-dish beams? In either case, time or evolution plays a role and would constrain the ages of the infrared-bright sources to less than a few $\times 10^4$ yr since evaporation. Interferometer data provide evidence for the presence of a separate physical component in the inner 1000 AU, but lack the spatial resolution to distinguish a shell from any remnant disk, for example on kinematic grounds.

An important difference between high- and low-mass objects may be the mechanism for the heating and dispersion of their envelopes. For low-mass YSOs, entrainment of material in outflows is the dominant process (Lada 1999). For intermediate-mass stars, outflows are important in the early phase, but ultraviolet radiation becomes dominant in the later stages (see § 3). The situation for high-mass stars is still unclear. The systematic increase in gas/solid ratios and gas-phase abundances point to global heating of the gas and dust, consistent with a radiative mechanism. However, a clear chemical signature of ultraviolet radiation on gas-phase species and ices in the embedded phase has not yet been identified, making it difficult to calibrate its effect. On the other hand, high-mass stars are known to have powerful outflows and winds, but a quantitative comparison between their effectiveness in heating an extended part of the envelope and removing material is still lacking. Geometrical effects are more important in less embedded systems, as is the case for low-mass stars, where the

circumstellar disk may shield part of the envelope from heating (Boogert et al. 2000b).

To what extent does the chemical evolution picture also apply to low-mass stars? Many of the chemical processes and characteristics listed in Table 1 are also known to occur for low-mass YSOs, but several important diagnostic tools are still lacking. In particular, sensitive mid-infrared spectroscopy is urgently needed to trace the evolution of the ices for low-mass YSOs and determine gas/solid ratios. Also, molecules as complex as CH_3OCH_3 and $\text{C}_2\text{H}_5\text{CN}$ have not yet been detected toward low-mass YSOs, although the limits are not very stringent (e.g. van Dishoeck et al. 1995). Evaporation of ices clearly occurs in low-mass environments as evidenced by enhanced abundances of grain-surface molecules in shocks (e.g. Bachiller & Pérez-Gutiérrez 1997), but whether a similar ‘hot core’ chemistry ensues is not yet known. Differences in the H/H_2 ratio and temperature structure in the (pre-)collapse phase may affect the grain-surface chemistry and the ice composition, leading to different abundances of solid CH_3OH , which is an essential ingredient for building complex molecules.

Future instrumentation with high spatial resolution ($< 1''$) and high sensitivity will be essential to make progress in our understanding of the earliest phase of massive star formation, in particular the SMA and ALMA at submillimeter wavelengths, and SIRTIF, SOFIA, FIRST and ultimately NGST at mid- and far-infrared wavelengths.

Acknowledgments. The authors are grateful to G.A. Blake, A.C.A. Boogert, A.M.S. Boonman, P. Ehrenfreund, N.J. Evans, T. Giannini, F. Lahuis, L.G. Mundy, A. Nummelin, W.A. Schutte, A.G.G.M. Tielens, and M.E. van den Ancker for discussions, collaborations and figures. This work was supported by NWO grant 614.41.003

References

- Adams, F.C., Lada, C.J. & Shu, F.H. 1987, *ApJ*, 312, 788
Bachiller, R. & Pérez-Gutiérrez, M. 1997, *ApJ*, 487, L93
Blake, G.A., Sutton, E.C., Masson, C.R., & Phillips, T.G. 1987, *ApJ*, 315, 621
Boogert, A.C.A., et al. 2000a, *A&A*, 353, 349
Boogert, A.C.A., et al. 2000b, *A&A*, submitted
Boogert, A.C.A., Helmich, F.P., van Dishoeck, E.F., Schutte, W.A., Tielens, A.G.G.M., & Whittet, D.C.B. 1998, *A&A*, 336, 352
Boonman, A.M.S., Wright, C.M. & van Dishoeck, E.F. 1999, in *The Physics and Chemistry of the Interstellar Medium*, eds. V. Ossenkopf et al. (Herdecke: GCA), 275
Boonman, A.M.S., et al. 2000a, in preparation
Boonman, A.M.S., et al. 2000b, in preparation
Carr, J., Evans, N.J., Lacy, J.H., & Zhou, S. 1995, *ApJ*, 450, 667
Caselli, P., Hasegawa, T.I., & Herbst, E. 1993, *ApJ*, 408, 548
Ceccarelli, C., Hollenbach, D.J. & Tielens, A.G.G.M. 1996, *ApJ*, 471, 400
Cernicharo, J., Lim, T., Cox, P., et al. 1997, *A&A*, 323, L25
Cesaroni, R., Felli, M., Testi, L., Walmsley, C., & Olmi, L. 1997, *A&A*, 325, 725
Cesaroni, R., Felli, M., Jenness, T., Neri, R., Olmi, L., Robberto, M., Testi, L., & Walmsley, C.M. 1999, *A&A*, 345, 949

- Charnley, S.B. 1997, *ApJ*, 481, 396
- Charnley, S.B. & Kaufman, M.J. 2000, *ApJ*, 529, L111
- Charnley, S.B., Tielens, A.G.G.M., & Millar, T.J. 1992, *ApJ*, 399, L71
- Charnley, S.B., Kress, M.E., Tielens, A.G.G.M., & Millar, T.J. 1995, *ApJ*, 448, 232
- Churchwell, E.B. 1999, in *The Origin of Stars and Planetary Systems*, eds. C.J. Lada & N.D. Kylafis (Dordrecht: Kluwer), 515
- Cummins, S.E., Linke, R.A., & Thaddeus, P. 1986, *ApJS*, 69, 819
- Dartois, E., d'Hendecourt, L., Boulanger, F., Jourdain de Muizon, M., Breittfeller, M., Puget, J.-L., & Habing, H.J. 1998, *A&A*, 331, 651
- Doty, S.D. & Neufeld, D.A. 1997, *ApJ*, 489, 122
- Ehrenfreund, P., van Dishoeck, E. F., Burgdorf, M., Cami, J., van Hoof, P., Tielens, A.G.G.M., Schutte, W.A., & Thi, W.F. 1998, *Ap&SS*, 255, 83
- Evans, N.J., Lacy, J.H., & Carr, J.S. 1991, *ApJ*, 383, 674
- Fuente, A., Martín-Pintado, J., Bachiller, R., Neri, R., & Palla, F. 1998, *A&A*, 334, 253
- Garay, G. & Lizano, S. 1999, *PASP*, 111, 1049
- Geballe, T.R. & Oka, T. 1996, *Nature*, 384, 334
- Giannini, T., et al. 2000, *A&A*, 346, 617
- Hartquist, T.W., Caselli, P., Rawlings, J.M.C., Ruffle, D.P., & Williams, D.A. 1998, in *The Molecular Astrophysics of Stars and Galaxies*, eds. T.W. Hartquist & D.A. Williams (Oxford: OUP), 101
- Harwit, M., Neufeld, D.A., Melnick, G.J., & Kaufman, M.J. 1998, *ApJ*, 497, L105
- Helmich, F.P. & van Dishoeck, E.F. 1997, *A&AS*, 124, 205
- Henning, Th., Burkert, A., Launhardt, R., Leinert, Ch., & Stecklum, B. 1998, *A&A*, 336, 565
- Hogerheijde, M.R., van Dishoeck, E.F., Salverda, J.M., & Blake, G.A. 1999, *ApJ*, 513, 350
- Ikeda, M. & Ohishi, M. 1999, in *IAU Symposium 197 Abstract Book, Astrochemistry: from molecular clouds to planetary systems*, 171
- Irvine, W.M., Goldsmith, P.F., & Hjalmarsen, Å. 1987, in *Interstellar Processes*, eds. D. Hollenbach & H.A. Thronson (Kluwer: Dordrecht), 561
- Jansen, D.J., Spaans, M., Hogerheijde, M.R., & van Dishoeck, E.F. 1995, *A&A*, 303, 541
- Jewell, P.R., Hollis, J.M., Lovas, F.J., & Snyder, L.E. 1989, *ApJS*, 70, 833
- Johansson, L.E.B., Andersson, C., Ellmér, J., et al. 1984, *A&A*, 130, 227
- Kuan, Y.J. & Snyder, L.E. 1994, *ApJS*, 94, 651
- Kulesa, C.A., Black, J.H., & Walker, C.K. 1999, *BAAS*, 194, 4709
- Lacy, J.H., Evans, N.J., Achtermann, J.M., et al. 1989, *ApJ*, 342, L43
- Lacy, J.H., Knacke, R., Geballe, T.R., & Tokunaga, A.T. 1994, *ApJ*, 428, L69
- Lada, C.J. 1999, in *The Origin of Stars and Planetary Systems*, eds. C.J. Lada & N.D. Kylafis (Dordrecht: Kluwer), 143
- Lahuis, F. & van Dishoeck, E.F. 2000, *A&A*, in press
- Langer, W.D., van Dishoeck, E.F., Blake, G.A., et al. 2000, in *Protostars and Planets IV*, eds. V. Mannings, A.P. Boss, & S.S. Russell (Tucson: Univ. Arizona), in press
- Liu, S.-Y. & Snyder, L.E. 1999, *ApJ*, 523, 683
- Lorenzetti, D., et al. 1999, *A&A*, 346, 604
- McCall, B.J., Geballe, T.R., Hinkle, K.H. & Oka, T. 1999, *ApJ*, 522, 338

- Millar, T.J. 1997, in *Molecules in Astrophysics: Probes and Processes*, IAU Symposium 178, ed. E.F. van Dishoeck (Dordrecht: Kluwer), 75
- Mitchell, G.F., Maillard, J.-P., Allen, M., Beer, R., & Belcourt, K. 1990, *ApJ*, 363, 554
- Motte, F., André, P., & Neri, R. 1998, *A&A*, 336, 150
- Nummelin, A., Bergman, P., Hjalmarsen, Å., Friberg, P., Irvine, W.M., Millar, T.J., Ohishi, M., & Saito, S. 1998, *ApJS*, 117, 427
- Ohishi, M. 1997, in *Molecules in Astrophysics: Probes and Processes*, IAU Symposium 178, ed. E.F. van Dishoeck (Dordrecht: Kluwer), 61
- Ohishi, M. & Kaifu, N. 1999, in *IAU Symposium 197 Abstract Book, Astrochemistry: from molecular clouds to planetary systems*, 143
- Ossenkopf, V. & Henning, Th. 1994, *A&A*, 291, 943
- Saraceno, P., Benedettini, M., Di Giorgio, A.M., et al. 1999, in *Physics and Chemistry of the Interstellar Medium III*, eds. V. Ossenkopf et al. (Berlin: Springer), 279
- Schilke, P., Groesbeck, T.D., Blake, G.A., & Phillips, T.G. 1997, *ApJS*, 108, 301
- Simon, R., Stutzki, J., Sternberg, A., & Winnewisser, G. 1997, *A&A*, 327, L9
- Sutton, E.C., Jaminet, P.A., Danchi, W.C., & Blake, G.A. 1991, *ApJS*, 77, 255
- Sutton, E.C., Peng, R., Danchi, W.C., et al. 1995, *ApJS*, 97, 455
- Turner, B.E. 1991, *ApJS*, 76, 617
- van den Ancker, M., et al. 2000a, *A&A*, submitted
- van den Ancker, M., et al. 2000b, *A&A*, in press
- van den Ancker, M., et al. 2000c, *A&A*, submitted
- van der Tak, F.F.S., van Dishoeck, E.F., Evans, N.J., Bakker, E.J., & Blake, G.A. 1999, *ApJ*, 522, 991
- van der Tak, F.F.S., van Dishoeck, E.F., Evans, N.J., & Blake, G.A. 2000a, *ApJ*, in press
- van der Tak, F.F.S. & van Dishoeck, E.F. 2000b, *A&A*, to be submitted
- van Dishoeck, E.F. 1998, *Far. Disc.*, 109, 31
- van Dishoeck, E.F. & Blake, G.A. 1998, *ARAA*, 36, 317
- van Dishoeck, E.F., Blake, G.A., Jansen, D.J., & Groesbeck, T.D. 1995, *ApJ*, 447, 760
- van Dishoeck, E.F. & Helmich, F.P. 1996, *A&A*, 315, L177
- van Dishoeck, E.F., Helmich, F.P., de Graauw, Th., et al. 1996, *A&A*, 315, L349
- van Dishoeck, E.F. & Hogerheijde, M.R. 1999, in *Origin of Stars and Planetary Systems*, eds. C.J. Lada & N. Kylafis (Dordrecht: Kluwer), 97
- van Dishoeck, E.F., et al. 1999, in *The Universe as seen by ISO*, eds. P. Cox & M.F. Kessler (Noordwijk: ESTEC), ESA SP-427, 437
- Waters, L.B.F.M. & Waelkens, C. 1998, *ARAA*, 36, 233
- Wright, C.M., van Dishoeck, E.F., Helmich, F.P., Lahuis, F., Boogert, A.C.A., & de Graauw, Th. 1997, in *First ISO Workshop on Analytical Spectroscopy*, ESA SP-419, 37
- Wright, C.M., van Dishoeck, E.F., Black, J.H., Feuchtgruber, H., Cernicharo, J., González-Alfonso, E., & de Graauw, Th. 2000, *A&A*, in press

Discussion

M. Ohishi: I agree with the point you mentioned, that the chemical differences among hot cores is due to a difference of evolutionary stage. Now we

have several well-known hot cores such as Orion KL/S, W 3 IRS5/H₂O/IRS4, Sgr B2 N/M/NW etc. Can you give us your personal view on the evolutionary differences of these sources?

E.F. van Dishoeck: Van der Tak et al. (2000a) argue that the infrared-bright objects such as W 3 IRS5 represent an earlier evolutionary phase than the hot cores, on the basis of an anti-correlation with the radio continuum. The physical picture is that the ionizing UV radiation and stellar winds push the hottest dust in the inner regions further out, decreasing the temperature of the dust and thus the near-infrared continuum. At the same time, the size of the region which can be ionized is increased. The 'erosion' of the envelopes thus occurs from the inside out. For other sources, infrared diagnostics are lacking, so that the situation is less clear. It would be great if chemistry could help to tie down the time scales of the various phases.

W. Irvine: How do you interpret the behavior of the PAH features as a function of evolutionary stage in the sources that you discussed?

E.F. van Dishoeck: The absence of PAH features in the early embedded stage can be due either to a lack of ultraviolet radiation to excite the features or to an absence of the carriers. Manske & Henning (1999, A&A, 349, 907) have argued for the case of Herbig Ae/Be stars that there should be sufficient radiation to excite PAHs in the envelope/disk system, so that the lack is likely due to the absence of the PAHs themselves. Perhaps the PAHs have accreted into the icy mantles at the high densities in the inner envelope and do not evaporate and/or are chemically transformed into other more refractory species on grains. Alternatively, the region producing ultraviolet radiation (H II region) may be very small in these massive objects, and the photons may not reach the PAH-rich material or have a very small beam filling factor. Once the envelope breaks up and ultraviolet radiation can escape to the less dense outer envelope, the PAH features from those regions will appear in spectra taken with large beams.

T. Geballe: You said that there is little evidence of the effect of ultraviolet radiation on solid-state chemistry. Isn't the 4.6 μm XCN feature a good example of that influence?

E.F. van Dishoeck: The 'XCN' feature is indeed the best candidate for tracing the ultraviolet processing of ices. If ascribed to OCN⁻, it likely involves HNCO as a precursor. In the laboratory, HNCO is produced by photochemical reactions of CO and NH₃, but in the interstellar medium grain surface chemistry is an alternative possibility which does not necessarily involve ultraviolet radiation (see Ehrenfreund & Schutte, this volume).

Y.C. Minh: Do you have an explanation of the low and constant abundances of CO₂ in the gas phase?

E.F. van Dishoeck: Charnley & Kaufman (2000, ApJ, 529, L111) argue that the evaporated CO₂ is destroyed by reactions with atomic hydrogen at high temperatures in shocks. This is an interesting suggestion, but needs to be tested against other species such as H₂O and H₂S which can be destroyed by reactions with atomic hydrogen as well. Also, the amount of material in the envelope that can be affected by shocks is not clear.